Biosensors and Bioelectronics 132 (2019) 90–96

Contents lists available at ScienceDirect

Biosensors and Bioelectronics

journal homepage: www.elsevier.com/locate/bios

# Towards integrated multi-sensor platform using dual electrochemical and optical detection for on-site pollutant detection in water

F. Sekli Belaïdi[a,b], L. Farouil[a,b], L. Salvagnac[a,b], P. Temple-Boyer[a,b], I. Séguy[a,b], J.L. Heully[c], F. Alary[c], E. Bedel-Pereira[a,b], J. Launay[a,b,*]

[a] CNRS, LAAS, 7 Avenue du Colonel Roche, F-31400 Toulouse, France
[b] Université de Toulouse, UPS, LAAS, F-31400 Toulouse, France
[c] LCPQ-IRSAMC, Université de Toulouse, 118 Route de Narbonne, F-31062 Toulouse, France

ARTICLE INFO

*Keywords:*
Compact fluidic platform
LED excitation
Electrochemical detection
Organic photo-detection.algal metabolism
Herbicide detection

ABSTRACT

The present work is dedicated to the development of a lab-on-chip (LOC) device for water toxicity environmental analysis and more especially herbicide detection. The final goal is focused on the functional integration of three-electrode electrochemical microcells (ElecCell) and organic photodetectors (OPD) in order to perform simultaneously electrochemical and optical detection in the frame of algal metabolism monitoring. Considering three different algae, ie. *Chlamydomonas reinhardtii*, *Pseudokirchneriella subcapitata* and *Chlorella vulgaris* while dealing with photosynthesis, the multi-microsensor platform enables to measure the variations of microalgae fluorescence as well as oxygen production. It is applied to study the Diuron herbicide influences on algal metabolism, evidencing fluorescence enhancement and oxygen production inhibition for concentrations as low as few tens of nanomoles. These results are performed with unconcentrated and six time concentrated algae solutions respectively, to estimate the ability of this dual-sensor system to conduct measurements without any sample preparation. Thus, according to the obtained results, the proposed LOC device is fully adapted to the electrochemical/optical dual detection for on-site pollutant analysis, ie. without sample pre-treatment.

## 1. Introduction

The effective management of water requires regular and continuous monitoring of quality to detect pollutants (nutrients, pesticides, and heavy metals) in order to prevent a serious threat to human health. Traditional monitoring techniques are generally based on laboratory analyzes of representative field-collected samples leading to considerable expenses. In addition, the standard available equipments are not portable. Therefore, the sample has to be collected directly on-site and even if best available transportation practices are applied, eg. freezing the samples, the composition could change during the drive to the lab producing false outcomes. Indeed, in large part, the quality of the analysis results is determined by the integrity of the samples sent to the laboratory. In this context, portable lab-on-chip (LOC) monitoring systems seem well suited to offer an attractive alternative way to proceed among the analytical methods actually available. Even, if care must be taken to protect samples from contamination or tampering, in situ measurement avoids those high risks. Otherwise, they save time, reduce reagent volume and costs. In fact, only samples showing too high level of contaminants should be carried and analyzed through classical laboratory tools to determine precisely the composition of the sample.

Over the two last decades numerous papers have been published on integrated LOC devices developed highlighting the efforts made and still to be done to reach real environmental applications. Jang et al. (2011), who detail the 1986–2010 state-of-the-art of lab-on-chip sensors for environmental water monitoring, conclude that the environmental monitoring sensor systems commercially available are either prohibitively costly or highly inflexible. They use invasive sampling that can alter chemical and biological conditions at the observation site; or they have electrodes that must be dipped into the water containing the pollutants. They propose an array of LOC incorporated into an automated analyzer with customized user interface to perform the continuous measurement for on-site applications. They convert a biochemical phenomenon into a detectable and measurable electrical signal proportional to the analyte concentration. Among papers cited by Jang et al. (2011), Brayner et al. (2011) show that whole cell biosensors and bioassays are a good candidate solution to satisfy the implemented requirements. More particularly, Fernandez-Jaramillo et al. (2012) give a review of general knowledge of real time measurements and provide

* Corresponding author at: CNRS, LAAS, 7 Avenue du Colonel Roche, F-31400 Toulouse, France.
*E-mail address:* jlaunay@laas.fr (J. Launay).

https://doi.org/10.1016/j.bios.2019.01.065
Received 26 October 2018; Received in revised form 21 December 2018; Accepted 29 January 2019
Available online 19 February 2019
0956-5663/ 

the necessary information to develop novel and custom biosensors for chlorophyll fluorescence measurement. They also emphasize that, as electronic devices are constantly evolving and becoming more efficient, equipment for measuring chlorophyll fluorescence will improve constantly in the same way. Indeed, various innovative and futuristic technologies have been developed between 2010 and 2015; Arduini et al. (2017) propose an exhaustive analysis of the literature of these technologies very useful for (bio)sensor effective environmental applications. Moreover, in this context, micro- and nano-fabrication technologies permit microsystems development including all components on board of the chip like LOC structure that could be an early and rapid warning system for on-site detection.

Very recently, Tahirbegi et al. (2017) report a miniaturized microfluidic device with integrated optical measurements for the in situ detection of pesticides by monitoring the metabolism of algae *Chlamydomonas reinhardtii*. This system uses three external optoelectronic instruments positioned on the bottom of the glass chip to measure oxygen, pH and algae fluorescence. Such a hybrid system will minimize the plug-and-play properties of this tool and the use of commercial components prevent to move towards flexible and tailor-made sensing systems.

The present work is focused on the one hand, on the electrochemical and fluidic improvements in order to simplify the first hybrid biosensor LOC prototype (Tsopela et al., 2014, 2016; Sekli Belaidi et al., 2016), which we have proposed. On the other hand, for further integration of optical transducers (dedicated to dual detection), we developed an organic photodiode (OPD) to measure the variations of the microalgae fluorescence. To evaluate performances of the whole tool, three green micro-algae strains are chosen as the biological sensing element: *Chlamydomonas reinhardtii* (Cr) for the electrochemical part, plus *Pseudokirchneriella subcapitata,* (Ps) and *Chlorella vulgaris* (Cv) for the optical one. Different media, with concentrated or un-concentrated algae solution, are prepared with toxic substances in order to study and to compare both electrochemical and optoelectronic sensors responses.

This paper demonstrates the utility of a standard multi-sensors platform using together the physical principles of electrochemistry and optic in a microfluidic system to allow fast and simple on-site complementary measurements for environmental applications. The different elements (fluidic structure with multi-channel for measurements, emission/reception with the optical devices, autonomous electrochemical microcells) are optimized, fabricated, tested and partially integrated on a unique platform. These dual-sensors allow the dual detection of chemical pollutants (pesticides) in fresh water thanks to the use of green micro-algae directly, with no added chemicals. This study is focused on the effects of Diuron herbicide on algae in order to compare the two aforementioned sensors characteristics. Indeed, Diuron is well known to enhance algae fluorescence and is often considered as a model pollutant for sensitivity qualification in a variety of detection platforms using algae as biosensors (Vedrine et al., 2003). The advantages of each kind of detection (electrochemical versus optical) are discussed in relation with the final application, which is the on-site detection of fresh water with no pretreatment.

## 2. Material and methods

### 2.1. Design of the lab-on-chip

The LOC platform, proposed in our previous work (Tsopela et al., 2014, 2016; Sekli Belaidi et al., 2016), consists in fluidic chambers integrating electrochemical sensors (in-situ) and chambers dedicated to optical fluorescence-based detection with optical devices stuck on the two sides of the chip. The new fluidic system, described here, is designed in order to ameliorate liquid injection, cleaning protocols and to reduce LOC costs thanks to, among others, the use of dry film resists (DFR) instead of the SU-8 photoresist used in previous SU-8 LOC, (Tsopela et al., 2016). The width of the channels was increased from 100 to 250 µm and the design of the chambers was changed from circular to ellipsoidal to facilitate its filling and to reduce the formation of bubbles inside channels. Eight independent detection chambers are designed on each platform enabling the simultaneous processing of different assays. The working electrodes have been hollowed out to make it semi-transparent to enhance light harvesting into the fluidic chamber and algae photosynthesis detection near the electrochemical sensor. Light emitting diodes (LED) and an organic photodiode (OPD) are disposed on each side of the fluidic chamber. The LEDs role consists in stimulating the algae (470 nm maximum emission is in accordance with green algae absorbance) to trigger the photosynthetic activity, responsible for oxygen and fluorescence production. OPD constitutes the other part of the optical detection system, which also includes excitation and detection filters. The purpose of these filters is respectively to avoid overlaying of LED spurious emission (see Fig. S1 Supporting information) and algae fluorescence signal, and to prevent excitation light to reach the OPD. So, reliable optical sensing integration, ie. without any device ageing, constitutes a very challenging step for those microsystems. Previously, electrochemical sensing experiments were successfully conducted with blue organic light emitting diodes (OLED) as light source (Tsopela et al., 2016). However, their efficiency could be quite not sufficient to ensure optical sensor reliability and repeatability since more light intensity is needed for algae fluorescence than for photosynthesis. Moreover, stable excitation filters, easy to integrate, represent another issue that we are currently addressing by developing micro-cavity OLED. So, at this stage of the study, integration will be confined to the detection part of the optical sensor, ie. the photodiode and detection filter. The structure of the LOCs is shown in Fig. 1.

### 2.2. Micro-fabrication of the lab-on chip

To begin the LOC fabrication process, the glass substrates are treated with oxygen plasma (800 W, 15 min) to enhance metal adhesion on glass surface. Titanium and platinum films (thickness: 12 nm and 120 nm respectively) are then sequentially thermally evaporated under vacuum ($P < 10^{-6}$ mbar) and patterned using a bilayer lift-off process. Afterward, to define the electrochemical microcell (ElecCell) including the working ultra-micro-electrodes (UME) array surrounded by the counter and reference electrodes, as well as the pads for electrical connection to the external devices, a sturdy and stable silicon nitride ($Si_3N_4$) insulation layer (thickness: 100 nm) is deposited by low temperature inductively-coupled plasma-enhanced chemical vapor deposition (IC-PECVD) (Vanhove et al., 2013). In the second phase of the LOC preparation, ie. the fluidic system, SU-8 photoresist is replaced by DFR, a negative dry film resist, DF 1050 (from EMS Adhesives). It consists in a 50 µm photosensitive layer laminated through a hot-roll laminator (Dynachem 350 h Laminator) with selected speed 0.5 m $min^{-1}$, temperature 100 °C, and pressure 2.5 bars. Despite its advantages (simple, fast and cheaper alternative to SU-8), the adhesion of DFR to the underlying wafer surface is of central importance for the durability of the patterned microfluidic system. In fact, delamination could be a catastrophic failure strongly depending on adhesion of the DFR film to the substrate. In order to enhance the adhesion to the under-laying $Si_3N_4$ film, a self-assembled monolayer (SAM) has been processed by immersion of the wafer into a mixture of 3-glycidyloxypropyl trimethoxysilane adhesion promoter using "$CO_2$ supercritic" thermodynamic conditions (60 °C, 120 bars). After this silanization step, the wafer is rinsed with ethanol, dried at 110 °C for 3 min and cleaned by the use of a 800 W oxygen plasma process just before lamination. Then, lamination is repeated five times to obtain the 250 µm resist thickness. Next, the resist is exposed to 240 mJ $cm^{-2}$ UV light using a mask aligner followed by a post exposure bake (PEB) at 100 °C for 15 min to obtain the fluidic structure. Finally, the resist is developed for 40 min in a commercially available cyclohexanon solution and the wafer is rinsed with deionized water and dried. At last, LOC cover is bonded and packaged according to the process defined by Tsopela et al.

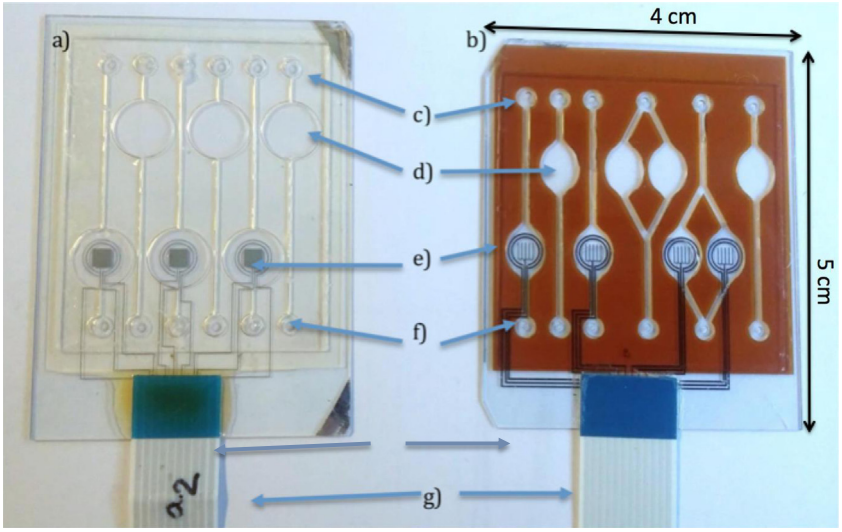


**Fig. 1.** Sensors platform obtained after packaging: a) First generation structure SU8-LOC, b) New structure DFR-LOC, c) Inlet, d) Optical chamber, e) Electrochemical chamber, f) Outlet, g) Electrical connections.

(2016).

This new fluidic structure, called DFR-LOC, provides a multi-parameter measurement tool using a unique chip with the complete electrochemical cells integrated in three of the chambers while the three others are dedicated to the fluorescence-based optical detection (see Fig. 1). The last two chambers are dedicated to blank samples for electrochemical and optical sensing. This matrix configuration also enables future integration of different algal species in order to increase sensor selectivity, as each species will be sensitive to different pollutant giving the possibility of managing multi-analysis.

### 2.3. Electrochemical sensor

In electrochemical sensing, the measured current is directly related to the concentration of the monitored specific specie in the tested liquid, by tuning the voltage value corresponding to the chemical reaction (oxidation or reduction) to be observed on the working electrode. The three-electrode electrochemical microcell (ElecCell) devices have been designed to avoid any current through the reference electrode: the working electrode is polarized thanks to the reference one and the current due to the oxidative/reduction reactions is collected through a counter electrode. The three metallic electrodes are prepared under vacuum by physical vapor deposition before the fluidic micro-fabrication process (Tsopela et al., 2016). Platinum or gold layers are deposited to create working and counter electrodes respectively while silver layer constitute the reference one. However, silver films obtained by evaporation techniques are thin (few hundreds of nanometers), thus fragile. Therefore, specific attention is required during the steps of the fluidic fabrication process (such as cleaning process using oxygen plasma which could irreversibly damage the silver layer, or during the $Si_3N_4$ deposition). Moreover, knowing that the reference electrode stability is directly related to the metal layer thickness, it is impossible to achieve stability with evaporated thin films. Furthermore, one of the advantages of DFR-LOC platform, compared to the SU8 one, is to allow performing different post process functionalization, like silver electroplating which will ensure a thick layer for the future reference electrode.

In the present study, the silver/silver chloride (Ag/AgCl) reference electrode is prepared after the fluidic network fabrication by electrodeposited silver and subsequent partial transformation to silver chloride. The platinum (see Section 2.2) is first preconditioned with an electrochemical protocol in sulfuric acid to improve adhesion and homogeneous deposition. The silver electroplating on platinum surface is accomplished from 0.3 M $AgNO_3$ in 1 M $NH_4OH$. The silver is deposited with a bias fixed at −20 mV versus Ag/AgCl/ Sat. KCl reference electrode at room temperature for 180 s and partially transformed to silver chloride in 1 M KCl solution by slow linear voltammetry at room temperature. The bias varies between 0.1 and 0.25 V vs. Ag/AgCl/Sat. KCl reference electrode with a speed fixed at 1 mV/s. SEM images of this electrode are shown in Fig. S1(a) (Supplementary information). The silver chloride, about 4 µm thick, consists in homogenous grains with a size ranging from one to two micrometers.

Even though silver chloride is often treated as an insoluble salt, it exhibits significant solubility in situations where the reference electrode is used for long-time applications. The dominating ageing factor is the complexation of silver chloride in the presence of chloride ions. In our case, long-time stability in an electrolyte with 0.1 M chloride ions is verified for several hours (see Fig. S1(b) in Supplementary information). It emphasizes that the electrodeposited AgCl is thick enough to provide a stable reference electrode for our application. In the same way, we optimize the detection properties of the working electrodes by post-process black-platinum (PtBl) deposited on platinum layers to obtain finally a three dimensions porous UME (Tsopela et al., 2014).

### 2.4. Optical sensor

As mentioned above, the optical sensor is made up of four independent elements: a LED, two optical filters and an OPD. The optical excitation includes a commercial blue LED (KP-3216QBC-D from Kingbright) and an excitation filter (ET470/40x from Chroma Technology Corp). On the over side of the fluidic platform, the integrated detection filter is formed of a simple commercial floating plastic sheet Roscolux (Supergel #19: R19 Fire) inserted between the OPD and the fluidic chamber. For the photodiode integration in the proposed system the prerequisite are the following: (i) high external responsivity matching with biosensor emission spectra, (ii) high specific detectivity which characterizes the capability to detect the weakest light signal, (iii) output signal must be linearly proportional to the input optical signal and (iv) a device size, ie. photon collection area, fitted on the microfluidic chambers design. Here, photodiode response time does not constitute a critical parameter for algae fluorescence measurements since in our case (continuous fluorescence monitoring) fast dynamic response is not required. In this field, OPD constitute a promising alternative to silicon-based photodetectors since they offer the ability to be processed directly on the LOC platform as close as possible to the algae. Moreover, they present high sensitivity in visible wavelength

range, low dark current and are cheap to manufacture (Kielar et al., 2016). The basic structure of an OPD is an organic heterojunction constituted of an electron donor (D) and an electron acceptor (A) sandwiched between metallic and transparent electrodes. In our system, the choice of D and A materials is fixed by algae maximum luminescence emission, eg. 680 nm. We choose the Poly[[4,8-bis[(2-ethylhexyl) oxy]benzo[1,2-b:4,5-b']dithiophene-2,6-diyl][3-fluoro-2-[(2 ethylhexyl)carbonyl]thieno[3,4-b]thiophenediyl]] (PTB7) as electron donor since this material has already shown high photovoltaic performances, a power conversion efficiency of 7.4% (Liang et al., 2010) and exhibited strong light harvesting between 350 and 750 nm, corresponding to the maximum chlorophyll emission. In our devices, contrary to what is usually chosen in organic solar cells, PTB7 is associated with $PC_{60}BM$ ([6,6]-phenyl-(C61)-butyric acid methyl ester) instead of $PC_{70}BM$ (([6,6]- phenyl-(C71)-butyric acid methyl ester) in order to limit the OPD photo-conversion between 400 and 550 nm (Sun et al., 2012). Glass substrates with indium tin oxide (ITO) anodes (CEC010S purchased from Praezisions Glas & Optik GmbH) were first patterned by means of photolithography and chemical etching such as to define the active area. Then the anodes are cleaned by sonication in successive baths of acetone, ethanol and isopropanol (10 min each). UV/ozone treatment of 10 min allowed the surface cleaning before the active layer deposition. PTB7 and $PC_{60}BM$ are dissolved in chlorobenzene with DIO co-solvent (3% v/v) to obtain 30 mg $mL^{-1}$ concentration solutions with D: A mass ratio of 1.5:1. The solution was stirred overnight at 50 °C. We fabricated optimized devices by spin-coating the solution at 750 rpm for 60 s in a $N_2$-filled glovebox to achieve a thickness of 180 nm. Finally, a 100 nm aluminum electrode is evaporated on top of the bulk heterojunction. At the end, devices with a 19.6 $mm^2$ photosensitive area size (adjusted to fluidic chambers) were encapsulated by a cavity cover glass and sealed with epoxy adhesive.

### 2.5. Bioassays

The green microalga *Chlamydomonas reinhardtii* (CC-125) (Cr) is obtained from Ecotoxicology of Aquatic Microorganisms Laboratory from the Quebecker "Département des Sciences Biologiques (GRIL – TOXEN, Université du Québec, Montréal, Canada). *Pseudokirchneriella subcapitata* (Ps) and *Chlorella vulgaris* (Cv) are obtained from the French "Laboratoire d'Ecologie des Hydrosystèmes Naturels et Anthropisés" (LHENA, Université Claude Bernard, Lyon France). Cr is cultivated in 200 mL Erlenmeyer flasks at 25 °C on mineral, liquid high salt medium (HSM) (Sueoka, 1960) with pH 6.9 ± 0.1 and Ps and Cv in Lefebvre-Czarda medium (Ionescu et al., 2006) with pH 7.0 ± 0.2. The cultures are aerated with the atmospheric air containing 2.5% (v/v) $CO_2$, which is passed through a bacteriological filter, and illuminated by white light with irradiance of 30 μE/$m^2$ s. The algal cells growth is synchronized by alternating light and dark periods (L/D − 14/10 h). Media and flasks are autoclaved (120 °C, 1.5 bar, 20 min) before inoculation and algal solutions are transplanted once a month under sterile conditions. Experiments are conducted with cells in the exponential growth phase. Two algae solutions are studied with $1 \times 10^6$ and $6 \times 10^6$ cells/mL, noted $C_1$ and $C_6$ respectively, to evaluate the detection properties of the electrochemical and optical sensors according to cell density. To obtain the $C_6$ concentration, 6 mL of initial algal suspension in the exponential growth phase, $C_1$, is centrifuged at 800*g* and re-suspended in 1 mL of the culture medium. The cells count is carried out by the Fast Read 102® (Gunetti et al., 2012), which is a plastic slide that allows the simultaneous reading of 10 chambers with a microscope.

## 3. Results and discussion

### 3.1. Electrochemical sensor validation

Following the microtechnological process, electrochemical characterization is conducted to validate the sensor. First, platinum thin layers were studied in a 0.1 M $H_2SO_4$ solution to compare the typical oxidative and reduction peaks during the cyclic voltammetry to the bare platinum reference curve. As previously demonstrated (Christophe et al., 2013), cyclic voltammograms representative of polycrystalline platinum were found (result not shown).

As described in the technical part 2.3, the functionalization of the microelectrodes is made post process: AgCl is formed as the reference electrode from a thick electroplated silver layer, and the collection surface of the working electrode is increased thanks to 3D PtBl deposit.

As the main chemical specie to be detected here is dissolved oxygen, we characterize the three-electrodes ElecCell devices with saturated, aerated and desaerated oxygen solutions at room temperature. Reduction current is observed from −0.7 V as expected (Tsopela et al., 2014). Future oxygen measurements related to algae photosynthesis are performed by chrono-amperometry at −0.8 V to guarantee the selective monitoring of oxygen on platinum electrode. As described previously (Tsopela et al., 2016), for herbicide detection using bio-electrochemical sensors, measurements are conducted by switching the light off and on to be able to determine: (i) the number of the active algae by the respiration slope during the dark period, (ii) the photosynthesis activity by monitoring the slope of the oxygen production during the light period. As those values are respectively estimated from the slopes of the on/off curves, 30 s for each period is found to be the sufficient and optimal time to obtain a fast sensing monitoring system. In this case, the integrated AgCl reference electrode is clearly stable enough for reliable measurements (see Section 2.3).

As electrochemical microcells (ElecCell) constitute very sensitive devices, one of the first requirements before toxicity measurements is to define the sensor optimum operating conditions. In fact, dissolved oxygen detection may be modified by temperature variations induced by LED lighting since oxygen diffusion coefficient is affected by temperature. Thus, oxygen variation slope versus LED intensity is studied for three fluidic chamber fillings: HSM pristine solution, $C_1$ *Chlamydomonas reinhardtii* in HSM, and $C_6$ *Chlamydomonas reinhardtii* in HSM (Fig. 2). Table 1 (see Supplementary information) represents the temperature enhancement regarding the LED luminance in LOC measurement configuration. Temperature variations as high as 8.8 °C have been determined, in the top of the microfluidic chamber (ie. opposite fluidic platform side regarding LED position) between light off and light on for LED maximum luminance of 7468 cd/$m^2$.

Since the LED used for photosynthesis is stuck to the LOC, the fluidic chamber is heated from 290 cd/$m^2$ incident lighting and lead to $O_2$ diffusion monitored by the electrochemical microcell even in HSM

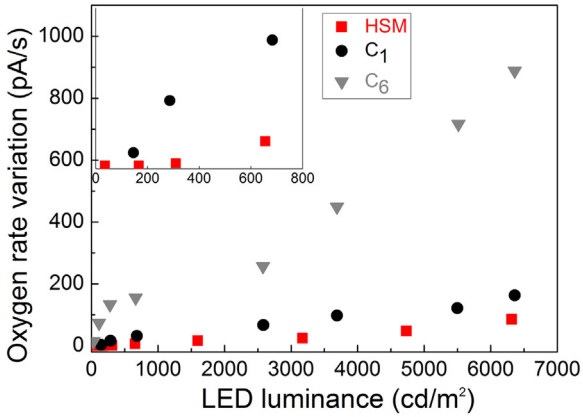


**Fig. 2.** $O_2$ rate variation versus LED intensity for three fluidic chamber fillings: HSM pristine solution (red square), $C_1$ Chlamydomonas reinhardtii in HSM (black circle), and $C_6$ Chlamydomonas reinhardtii in HSM (gray triangle). Inset, zoom for HSM pristine solution and C1 in HSM in the range 0–800 cd/$m^2$ LED intensity. (For interpretation of the references to color in this figure legend, the reader is referred to the web version of this article).

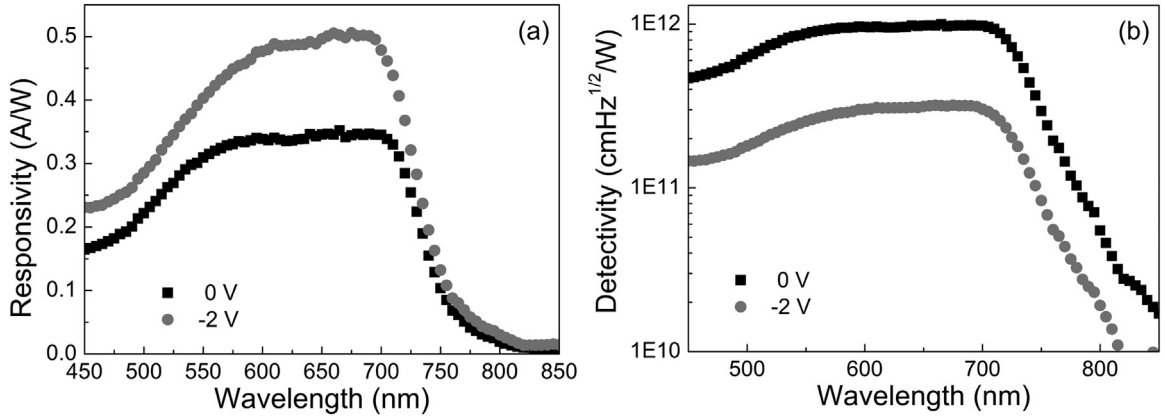


**Fig. 3.** Responsivity (a) and detectivity (b) of the developed organic photodetector.

solution for 700 cd/m$^2$ (see inset Fig. 2). Finally, optimal LED luminance value chosen in order to avoid sensor transduction alteration is estimated to 290 cd/m$^2$. This latest value is fixed for all toxicity assays performed by chrono-amperometry thereafter.

### 3.2. Optical sensor validation

The responsivity R and specific detectivity D* of the OPD described Section 2.4 are depicted in Fig. 3. The OPD characterization has been performed at 0 and −2 V. This OPD display a significant response in terms of responsivity and detectivity between 550 and 750 nm. At 680 nm, the wavelength corresponding to chlorophyll maximum emission, the OPD responsivity is 0.38 and 0.5 A/W for 0 and −2 V bias respectively, which is close to the values reported for standard commercial photodiodes. The specific detectivity shows a maximum for the unbiased device at $10^{12}$ cm Hz$^{1/2}$/W.

We followed the evolution of detectivity D* for the devices developed here according to their active area from 3 to 19.6 mm$^2$. We have noticed no significant changes in those performances (not shown). This result leads to the choice of the biggest device in order to collect the maximum of the biosensor emission. Considering that the expected algae fluorescence will be very weak, the focus is on the OPD detectivity rather than on its sensitivity. As seen in the Fig. 3b, applying a reverse bias subsequently lowers D* values. The reason for this is the rising dark current with voltage in PTB7/$PC_{60}$BM photodiodes. So, in order to enhance the sensor detection range, further micro-algae fluorescence measurements will be realized at zero bias.

Experimental data of photocurrent versus intensity of the incident light at 650 nm, for the device studied, is shown in Fig. 4. There should be a linear dependence with respect to incident light intensity, at 0 V and it is verified for at least 4 orders of magnitude. The lowest detectable light intensity is 3.3 nW/cm$^2$, which is consistent with the fluorescence signal measured for algae in growth phase (in culture medium) with a 2600 cd/m$^2$ blue LED.

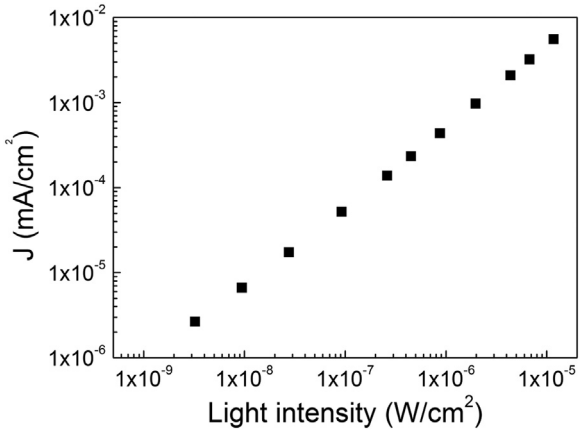


**Fig. 4.** Photocurrent density as a function of the light intensity at 650 nm, the minimum range is equivalent to algae fluorescence.

In order to assess our optical sensor response versus algae cells density (the three algae strains are evaluated), we compare algae fluorescence signal obtained on the two algae solutions $C_1$ and $C_6$ without pollutant. The signal is recorded continuously (see Fig. S.3 Supplementary information) at room temperature with the developed OPD. The measurements consist in realizing cycles of darkness and light of one minute each repeated three times for two LED intensities, 2600 and 6350 cd/m$^2$ respectively (2600 cd/m$^2$ corresponding to the lowest LED luminance allowing flurorescence signal measurement with our system, and 6350 cd/m$^2$ to the value used by other groups in similar sensing platforms (Lefèvre et al., 2012). As expected, for algae suspension from the culture $C_1$, photocurrent enhancement is less pronounced than for the $C_6$ samples, as shown on Fig. 5. These signals are exacerbated when using 6350 cd/m$^2$ blue light as excitation source, which demonstrated a highest level of fluorescence variation between $C_1$ and $C_6$, especially for Cr and Ps micro-algae. Since, maximum photocurrent values are recorded with $C_6$ solutions of Cr and Ps for 6350 cd/m$^2$ LED lighting, further measurements involving optical sensor will be carried out, under those experimental conditions in terms of algae strains, concentration and LED luminance.

### 3.3. Herbicide detection using dual microsensors

To validate and compare the microsystem sensors in the presence of a pollutant, we studied the inhibition of photosynthetic activity in the presence of Diuron herbicide. Indeed, Diuron herbicide is well known to have an effect on PSII leading to an immediate impact upon chlorophyll A fluorescence yield together with $O_2$ production inhibition (Govindjee, 1995). Two different algae solutions, $C_1$ and $C_6$, are set without and with pesticide (Diuron, *Sigma-Aldrich*, 98% purity). The pesticides concentrations were prepared in the 0 – 1 µM range to fit with environmental application.

Diuron is dissolved in ethanol (ethanol, HPLC grade, *Fischer Scientific*, 99,99% purity) due to its low solubility in water (42 mg L$^{-1}$ at 20 °C). In turn, the nominal concentrations of each solution tested were obtained by dilution of the stock solution in culture medium. Ethanol solutions containing Diuron are mixed with algal test solutions re-suspended in culture medium in order to prepare final solutions of various Diuron concentrations (from 0 to 1 µM). Samples to be measured are then injected in the detection chambers with a simple syringe for electrochemical and optical monitoring since the microfluidic structure hydrophilic properties prevent from the use of a micro-pump.

The optical part of the biosensor is first tested in the presence of this

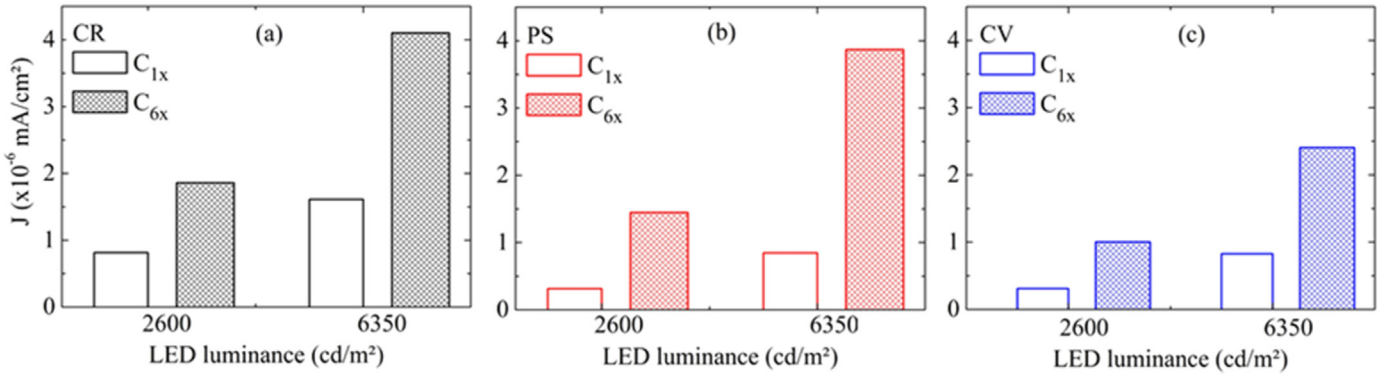


**Fig. 5.** OPD current density monitored for three algae strains, (a) CR, (b) PS and (c) CV pristine solutions $C_1$ and concentrated ones $C_2$ for two LED intensities, 2600 cd/m$^2$ and 6350 cd/m$^2$.

herbicide for Cr and Ps algae strains. After a contamination time of 15 min, the algae fluorescence rate is detected according to the procedure described above (Section 3.2). Fluorescence variations are expressed as a percentage given by the equation displayed by Gosset et al. (2018).

$$FE(\%) = \frac{Fs - Fc}{Fs} x100$$

where FE is the fluorescence enhancement (in %), Fs is the fluorescence signal acquired for algae exposed to Diuron (in mA/cm$^2$), and Fc the fluorescence signal for control algae (in mA/cm$^2$).

Fig. 6.(a) illustrates the fluorescence signal changes as a result of herbicide addition: the two algae appeared to be sensitive to Diuron exposure. An increase of these signals with the concentration of herbicide is observed. By far, for optical sensing, the most sensitive specie is Ps with an estimated early Diuron detection of 10 nM (20 nM for Cr).

A good correlation is obtained between those dose-response curves and those displayed by Gosset et al. (2018) performed on the same microalgae strains. However, the main advantages of the optical sensor studied here is its limit of detection which is of the order of some tens of nanomoles, similar to the LOD determined by Lefèvre et al. (2012) in the same kind of systems using OLED and OPD. At first glance, this result is due to position-related optical devices in close proximity to the fluidic chamber containing the algae.

As described in the 3.1 part, dark and light periods were applied on an algae solution containing different pollutant concentrations. First of all, the slope of the oxygen reduction curve, obtained by chrono-amperometry technique, leads to the production of oxygen by algae (minus the respiration) when the light is on. To be able to compare each slope value versus pollutant concentration, we have to estimate very precisely the quantity of active algae responsible of the photosynthesis process, which can be different from the total number of algae obtained with a classical cell counter. For this purpose, we monitor the respiration slope during the dark period to determine the equivalent number of "alive" algae before switching the light on for the photosynthesis process. In fact, it is assumed that pollutants have no effect on the respiration phase. We use this quantification and mathematical treatment to determine the oxygen production rate versus Diuron concentration in different solutions added to algae culture. Linear response is observed (Fig. 6(b)) in a large range of herbicide concentration (0.1–1 µM), and Diuron can be measured with a concentration range down to 0.1 nM even with the unconcentrated algae solution ($C_1$). In fact, no further tests using $C_6$ solution have been conducted as the detection properties related to the variation of oxygen production is representative enough with $C_1$ solution. So, we point out that for future in-situ use, no biosensor pre-treatment will be required to proceed to the electrochemical measurements.

The results obtained using the electrochemical microcell (ElecCell) show a large sensitivity (92% $O_2$ inhibition/µM) for Diuron detection over an extensive range, compatible with legal acceptable concentrations in the frame of environmental analysis. Compared to previous works (Tsopela et al., 2014, 2016) a linear variation is found for the highest Diuron concentrations (> 0.1 M) whereas an enhanced inhibition is evidenced for the lowest ones (< 0.1 M). Since amperometric response of the PtBl ultra-micro-electrode array is known to be linear, such phenomenon should be related to the *Chlamydomonas reinhardtii* micro-algae metabolism. Indeed, as previously discussed, we are analyzing a low algae concentration solution in order to estimate the possibility of working easily with our system. Therefore, when we look at the influence of Diuron on the photosynthetic activity of algae,

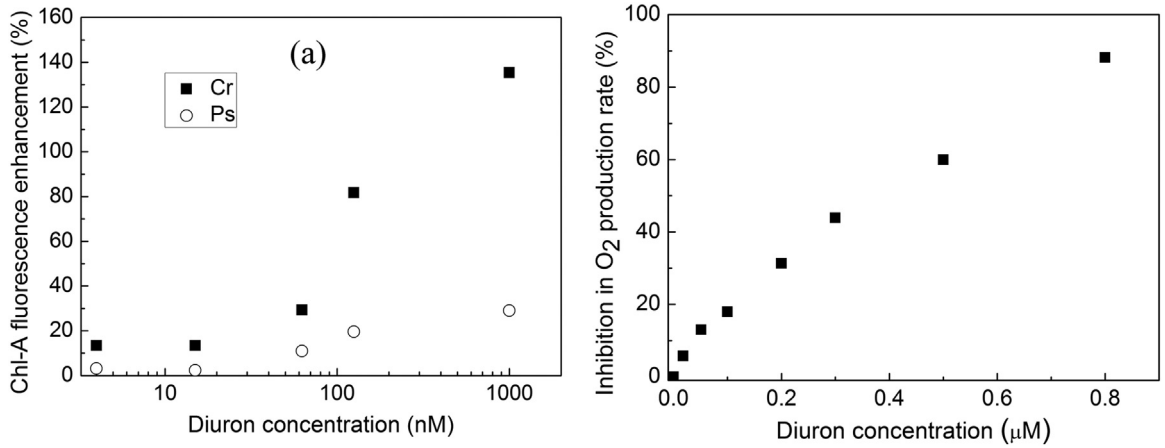


**Fig. 6.** a) Optical biosensor response curves for two algae strains (Cr and Ps), $C_6$ solutions, (b) Impact of Diuron concentration on Cr $O_2$ production rate ($C_1$ solution).

the inhibitory effect is visible very early on the response curve, ie. for very low concentrations of pollutant. This effect is increased tenfold by the fact that we work in micro-volume. This is expressed by a slope variation on the response curve (Fig. 6), as the Diuron concentration increases, showing a progressive saturation of the detection. It can therefore be seen that at a concentration of approximately 1 µM, the inhibition rate on such a low algae solution is already close to 100%.

The combined sensors presented in this paper demonstrate their ability to be used as an indicator of the photosynthetic activity of micro-algae biosensors, and highlight a couple method of herbicide assay. If the biological element studied is the same for the two sensors, the physiological parameters and transduction signals monitored differs. The detection limit, estimated from electrochemical measurements is a hundred times greater than that obtained with the optical sensor in the same fluidic platform. These discrepancies may stem from three factors including the nature of the measured physiological parameters (combined with two types of signal transduction), the difference in the algal concentration used for toxicity assays and the sensors sensitivity. Indeed, when using optical detection, the recorded signal consists in raw photocurrent density which has not undergone either amplification or signal processing. So, although this paper relates the coupled herbicide dual-detection with state-of-the-art devices, significant improvements will be obtained by further integration of the optical part of this system combined with signal processing. In addition, it should allow working with $C_1$ solution for both detection principle (electrochemical/optical), namely without any biosensor pre-treatment, as it is already the case with the electrochemical sensor.

Another important outcome lies here in the ability to achieve pollutant selectivity, which is very difficult to obtain by using a single transduction system. Since chlorophyll A fluorescence is almost entirely due to Photosystem II (PSII) function targeted by several classes of herbicides (Diuron, diazines, triazine, phenols…) (Giardi et al., 2005), the dual-sensor proposed should provide a way to discriminate some toxic chemical species.

## 4. Conclusion

A portable lab-on-chip device is developed for water toxicity environmental analysis and more especially herbicide detection. In order to provide complementary analysis, a dual sensor platform is implemented while considering both electrochemical optical detections. As a result, developing a new fluidic packaging technology based on the use of dry film resist (DFR), three-electrode electrochemical microcells (ElecCell) and an organic photodetectors (OPD) lead, in a functional way, to a DFR-LOC fully adapted to liquid phase analysis. Demonstration is performed through the study of algal photosynthetic metabolisms by using three different algae, ie. *Chlamydomonas reinhardtii*, *Pseudokirchneriella subcapitata* and *Chlorella vulgaris*, and dealing with Diuron herbicide. Thus, the Diuron concentration increase is found to be responsible for an algal oxygen production inhibition as well as an algal red fluorescence enhancement. Finally, it is demonstrated that (i) the ElecCell and LED/OPD microsensor technologies are successfully adapted to the analysis of algae metabolisms, and (ii) that the associated DFR-LOC device is fully adapted to the electrochemical/optical dual detection for on-site pollutant analysis, ie. without sample pre-treatment. Fully optical integration, that involves micro-cavity OLED as excitation light and OPD as detection device, is under progress. It will increase the optical sensor sensitivity. Further works will therefore imply the development of multi-algae/multi-sensor lab-on chip in order to deal with the selective detection of different pollutants, ie. different herbicides in a frame of a "plug-and-play" system for water analysis.

## Acknowledgement

The authors would like to thank the French "Agence Nationale de la Recherche" (ANR, project DOLFIN, n°ANR-13-JS03-0005-01) for financing the project. Furthermore, microfabrication procedure was partly supported by the French RENATECH network.

## Appendix A. Supporting information

Supplementary data associated with this article can be found in the online version at doi:10.1016/j.bios.2019.01.065.

## References

Arduini, F., Cinti, S., Scognamiglio, V., Moscone, D., Palleschi, G., 2017. Anal. Chim. Acta 959, 15–42.
Brayner, R., Couté, A., Livage, J., Perrette, C., Sicard, C., 2011. Anal. Bioanal. Chem. 401, 581–597.
Christophe, C., Sékli Belaïdi, F., Launay, J., Gros, P., Questel, E., Temple-Boyer, P., 2013. Sens. Actuators B 177, 350–356.
Fernandez-Jaramillo, A.A., Duarte-Galvan, C., Contreras-Medina, L.M., Torres-Pacheco, I., Romero-Troncoso, R., de, J., Guevara-Gonzalez, R.G., Millan-Almaraz, J.R., 2012. Sensors 12, 11853–11869.
Giardi, M.T., Guzzella, L., Euzet, P., Rouillon, R., Esposito, D., 2005. Environ. Sci. Technol. 39, 5378–5384.
Gosset, A., Durrieu, C., Renaud, L., Deman, A.-L., Barbe, P., Bayard, R., Chateaux, J.F., 2018. Biosens. Bioelectron. 117, 669–677.
Govindjee, 1995. Aust. J. Plant Physiol. 22, 131–160.
Gunetti, M., Castiglia, S., Rustichelli, D., Mareschi1, K., Sanavio, F., Muraro, M., Signorino, E., Castello, L., Ferrero, I., Fagioli, F., 2012. J. Transl. Med. 10, 112–123.
Ionescu, R.E., Abu-Rabeah, K., Cosnier, S., Durrieu, C., Chovelon, J.M., Marks, R.S., 2006. Electroanalysis 18, 1041–1046.
Jang, A., Zou, Z., Kug Lee, K., Ahn, C.H., Bishop, P.L., 2011. Meas. Sci. Technol. 22, 1–18.
Kielar, M., Dhez, O., Pecastaings, G., Curutchet, A., Hirsch, L., 2016. Sci. Rep. 6 (39201), 1–11.
Lefèvre, F., Chalifour, A., Yu, L., Chodavarapu, V., Juneau, P., Izquierdo, R., 2012. Lab Chip 12, 787–793.
Liang, Y., Xu, Z., Xia, J., Tsai, S.-T., Wu, Y., Li, G., Ray, C., Yu, L., 2010. Adv. Mater. 22 (E135-E138).
Sekli Belaidi F., Tsopela A., Salvagnac L., Ventalon V., Bedel-Pereira E., Bardinal V., Seguy I., Temple-Boyer P., Juneau P., Izquierdo R., Launay J., 2016. IEEE-NMDC, Nanotechnology Materials and Devices Conference, 9-12 October in Toulouse France, 2016.
Sueoka, N., 1960. Proc. Natl. Acad. Sci. USA 46, 83–91.
Sun, Y., Welch, G.C., Leong, W.L., Takacs, C.J., Bazan, G.C., Heeger, A.J., 2012. Nat. Mater. 11, 44–48.
Tahirbegi, I.B., Ehgartner, J., Sulzer, P., Zieger, S., Kasjanow, A., Paradiso, M., Strobl, M., Bouwes, D., Mayr, T., 2017. Biosens. Bioelectron. 88, 188–195.
Tsopela, A., Lale, A., Vanhove, E., Reynes, O., Seguy, I., Temple-Boyer, P., Juneau, P., Izquierdo, R., Launay, J., 2014. Biosens. Bioelectron. 61, 290–297.
Tsopela, A., Laborde, A., Salvagnac, L., Ventalon, V., Bedel-Pereira, E., Seguy, I., Temple-Boyer, P., Juneau, P., Izquierdo, R., Launay, J., 2016. Biosens. Bioelectron. 79, 568–573.
Vanhove, E., Tsopéla, A., Bouscayrol, L., Desmoulins, A., Launay, J., Temple-Boyer, P., 2013. Sens. Actuators B 178, 350–358.
Vedrine, C., Leclerc, J.C., Durrieu, C., Tran-Minh, C., 2003. Biosens. Bioelectron. 18, 457–463.